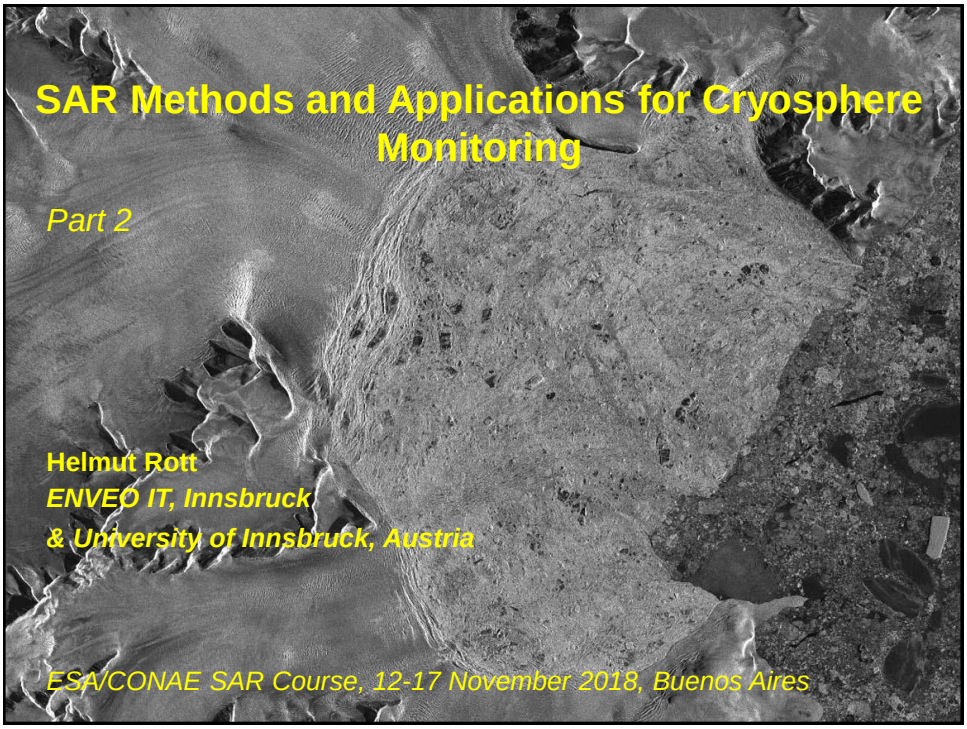

Contents of the Lecture

1. Overview on Approaches for Studying Dynamics and Mass Balance of Glaciers and Ice Sheets
2. Interferometric Volume Decorrelation and Scattering Phase Centre in Snow and Ice
3. Ice Motion Retrieval by InSAR and Image Correlation Techniques
   - InSAR Method for Glacier Velocity
   - Application Example: Flow Acceleration and Water Outbreak
   - Offset Tracking Method for Glacier Motion and Products
   - Mass Balance by Input/Output Method
   - Retrieval of 3D Ice Motion
4. Single-Pass InSAR Surface Elevation Change and Mass Balance
   - Study on InSAR Penetration Bias
   - SP-InSAR DEM Differencing – Antarctic Peninsula & Patagonia
5. Glacier Tomography by Airborne L-band InSAR

Ice Flow and Mass Transport on a Glacier

Ice motion of glacier in equilibrium state

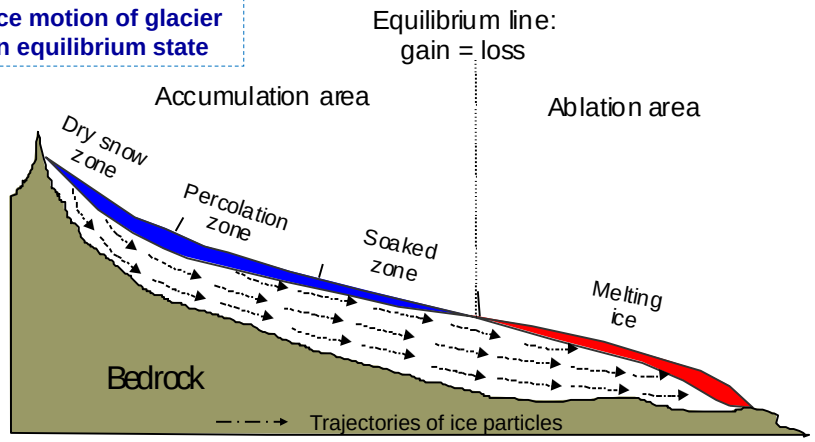

Objectives for mapping and monitoring Ice Motion:

- **Understanding the processes of glacier flow and impact of external forcing**
- **Analyzing and predicting glacier response to climate change**
- **Retrieving ice export by calving (Input/Output method for mass balance)**

Mass Balance and Ice Export of a Marine Ice Sheet

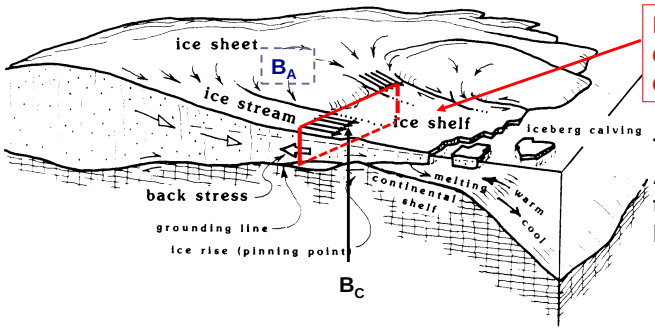

Ice shelf (in)stability is critical for mass balance of grounded ice

The main export of Antarctic ice is routed through ice shelves and lost by iceberg calving.

$$B_c = \int_Y [\bar{u}(y)H(y)]dy$$

The contribution to sea level rise is determined by imbalance of net accumulation, B_A, on grounded ice minus the export through a cross section at the grounding line or calving front, B_C.

Total net mass balance $\mathbf{B_N = B_A - B_C}$

Input/Output Method IOM: Computes the net balance B_n as difference between B_A (net surface mass balance SMB) and calving flux B_c

Satellite Applications for Surface Elevation Change and Mass Balance of Glaciers and Ice Sheets

- **Measurement of surface elevation change (Altimetry, DEM differencing)**
  - ★ Measures elevation change over time, converts volume to mass change
  - → Critical issue for mass balance estimate: Accounting for changes in firn layer thickness or density for relating volume to mass
- **Input-Output Method (IOM)**
  - ★ Net balance B_n at basin scale, as difference between surface mass balance SMB (B_{ac} + B_{ab})→ and flux B_{cv} across frontal gate

$$B_n(\Delta t) = B_{ac} + B_{ab} - B_{cv} = \int_{S_{ac}} b_n dS + \int_{S_{ab}} b_n dS - \rho \int_y [u_{cv}(y) h(y)] dy = \langle b_n \rangle S - B_{cv}$$

SMB

  - ★ Surface velocity by repeat-pass InSAR
  - → Critical issues: knowledge of SMB and cross section at flux gates
- **Gravimetry** (GRACE, GOCE)
  - ★ Measures of temporal changes of gravity field, directly related to mass changes. Regional solutions by parameterization of local mass variations as mass concentrations (mascons)
  - → Critical issues: Correction for Glacial Isostatic Adjustment (GIA), spatial leakage, low spatial resolution

Interferometric Coherence in Snow and Ice

Degree of coherence:

$$\gamma_{total} = \gamma_{SNR} \cdot \gamma_{surface} \cdot \gamma_{volume} \cdot \gamma_{temporal}$$

$$\gamma = \frac{\left| E\{V_1 V_2^*\} \right|}{\sqrt{E\{V_1\}^2 E\{V_2\}^2}}$$

Time dependent factors for decorrelation $\gamma_{temporal}$:

- Surface melt
- Snowfall
- Snow drift (wind erosion and deposition)

These are main obstacles for repeat-pass InSAR over snow and ice

Other factors

- Volume wavenumber shift (volume decorrelation in dry, deep snow; dependent on baseline) γ_{volume}
- Surface wavenumber shift (dependent on baseline) $\gamma_{surface}$
- Thermal noise (relevant for low σ°) γ_{SNR}

Temporal and Volume Decorrelation in Snow and Ice

Decorrelation due to melting

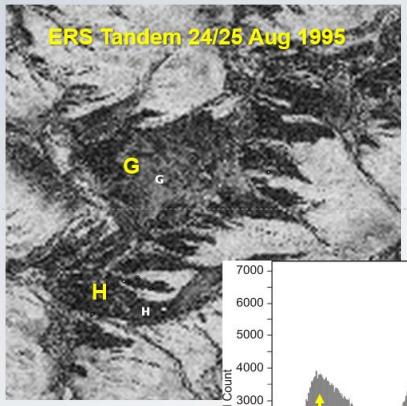

Ötztal Glaciers

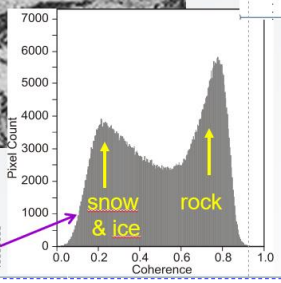

Wet snow

Volume Decorrelation in **dry snow**

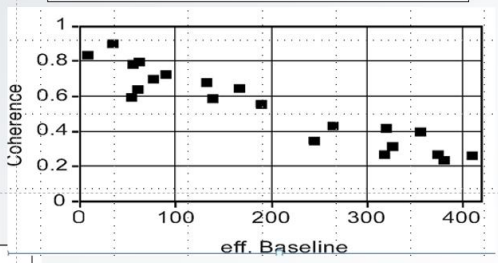

Coherence decreases with increasing length of InSAR baseline

From 3-day repeat pass ERS-1 SAR data, Antarctic inland ice (Dronning Maud Land)

← Temporal decorrelation: See also Part 1, slide 39

InSAR Application for Mapping Glacier Motion

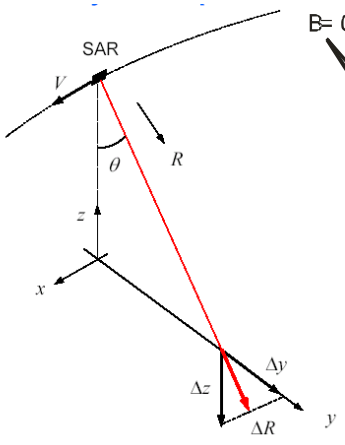

Across track view

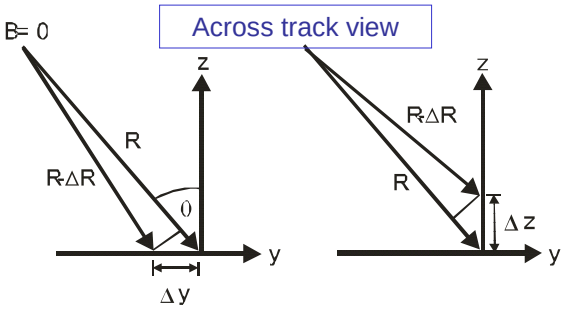

$\Delta\phi_{dis} = (4\pi/\lambda)\Delta R = (4\pi/\lambda)(\Delta y \sin\theta - \Delta z \cos\theta)$

InSAR measures the displacement in LOS of the radar beam

C-band SAR (λ = 5.66 cm):
$\Delta\phi\ (2\pi) \Rightarrow \Delta R =$ 2.83 cm

L-band SAR (λ = 25 cm):
$\Delta\phi\ (2\pi) \Rightarrow \Delta R =$ 12.50 cm

X-band SAR (λ = 3.12 cm):
$\Delta\phi\ (2\pi) \Rightarrow \Delta R =$ 1.56 cm

TerraSAR-X Interferogram

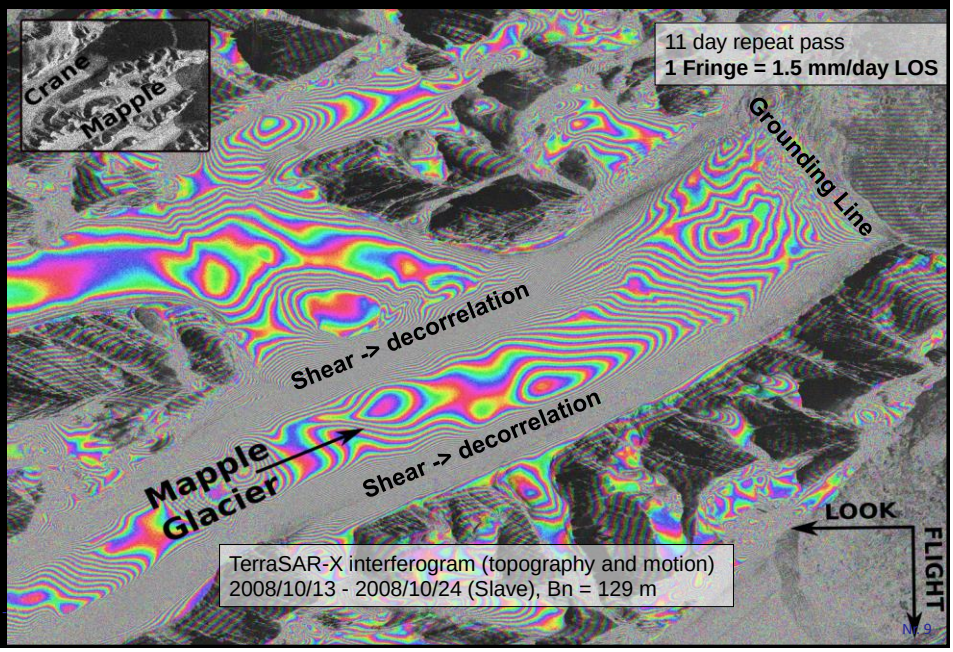

Referring InSAR Displacement to Glacier Motion

- **InSAR from single track yields the LOS component of velocity**
- **For ice dynamics modelling the 3-D velocity vector is needed**
- **3 interferometric observations from independent directions are needed to obtain the true velocity vector**

General 3D motion:

$$\mathbf{v} = v_x\hat{\mathbf{x}} + v_y\hat{\mathbf{y}} + v_z\hat{\mathbf{z}} = \mathbf{v}_h + v_z$$

$\mathbf{v}_h$ horizontal velocity vector

$$\text{InSAR phase in LOS}: \phi_2 - \phi_1 = \frac{4\pi}{\lambda}\Delta R$$

Figure assumes **motion across track** ($v_x = 0$):

$$\phi_2 - \phi_1 = \frac{4\pi}{\lambda}\left[v_y \sin\theta - \left(\frac{\partial S}{\partial t} + v_y\frac{\partial S}{\partial y}\right)\cos\theta\right]$$

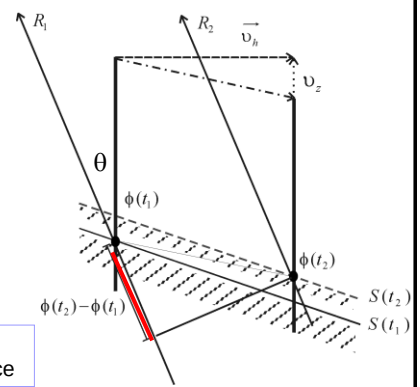

∂S/∂t = w + b local surface displacement
w - vertical particle velocity; *b* – surface mass balance

3-D Ice-Velocity with Surface-Parallel Flow Assumption

***Single pass InSAR, Surface-parallel flow**: LOS displacement is projected onto surface in direction of maximum slope*

Surface parallel flow: $\frac{\partial S}{\partial t} = \mathbf{n_S} \cdot \mathbf{v} \;\; ; \;\; \mathbf{n_S} = (-\frac{\partial S}{\partial x}, -\frac{\partial S}{\partial y}, 1)$

$$\mathbf{v} = \mathrm{v}_x \frac{\partial}{\partial x} S(x,y) + \mathrm{v}_y \frac{\partial}{\partial x} S(x,y) + \mathrm{v}_z = \mathbf{v}_h + \mathrm{v}_z = \mathbf{v}_h + \left[\nabla_{xy} S(x,y)\right]^T \mathbf{v}_h$$

This assumption introduces errors for glaciers that are not in equilibrium (e.g. surging glaciers)

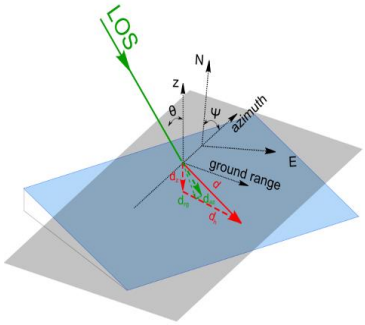

Improved estimation of $\mathbf{v}_h$ if InSAR pairs of **ascending and descending orbits** available

$$\mathbf{v}_h = \mathrm{v}_a \hat{\mathbf{n}}_a + \mathrm{v}_d \hat{\mathbf{n}}_d$$

a – ascending orbit
d – descending orbit

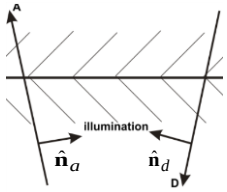

InSAR Observations of Changes in Glacier Flow

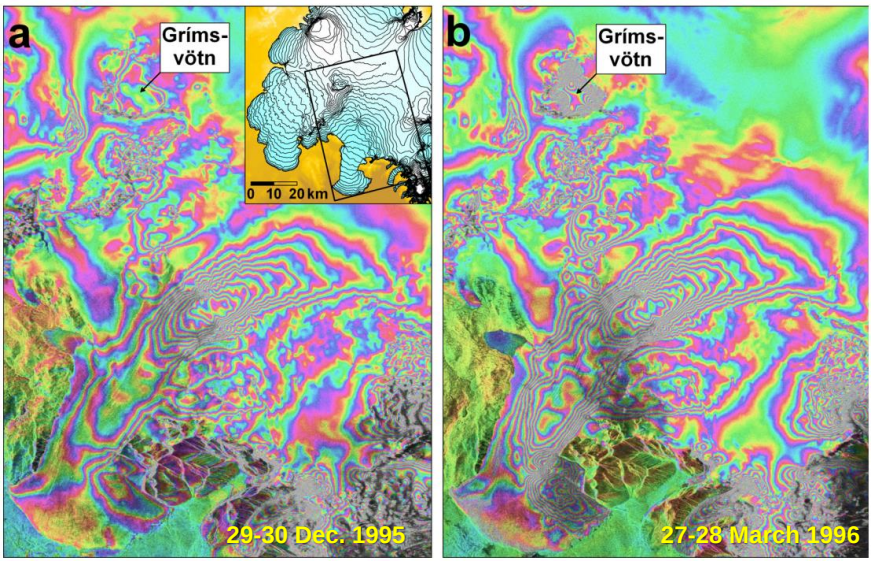

→ Radar LOS Motion-related interferograms

Glacier Acceleration as Precursor to Water Outbreak

Skeidararjökull - Vatnajökull, Iceland

Flow direction by combining ascending and descending interferograms

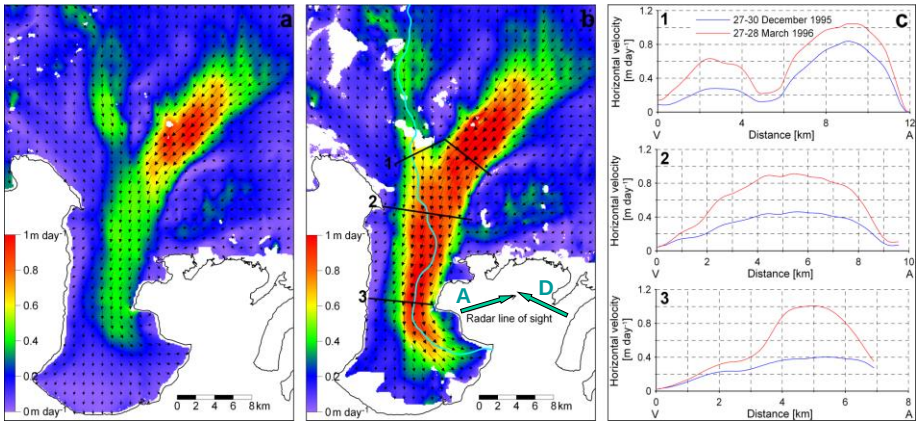

29-30 December 1995 27-28 March 1996

E. Magnusson, H. Rott, H, Björnsson, J. Glaciol. 2007

Water Accumulation in Initial Phase of Jökulhlaup

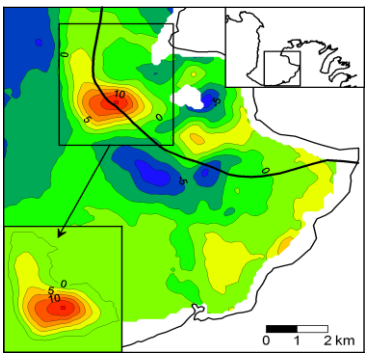

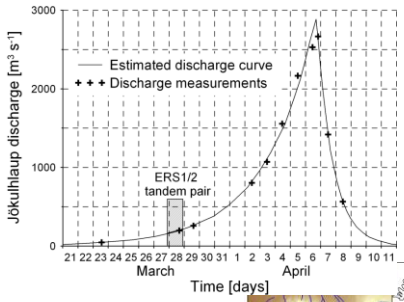

Computed from InSAR Analysis, 27-28 March 1996 and ice dynamic model.

Local uplift due to water accumulation: 0.35 Mill. m^3/24 h.

The InSAR analysis provides new insights in glacier hydraulics – potential for early warning

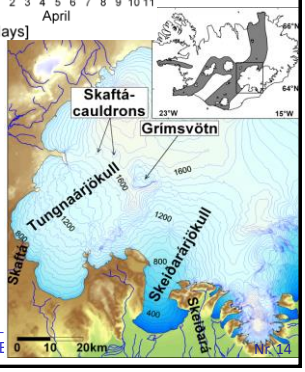

SAR Offset Tracking Techniques for Ice Motion

Basic principle: Matching of image templates by cross correlation (along track and in range) in co-registered SAR images.

Possibilities for features to be tracked:

1. **Amplitude correlation**: Uses persistent features in backscattering amplitude images (e.g. crevasses, drainage features). Advantage: Coherence not required. Disadvantage: Lack of features in accumulation areas of glaciers (snow areas) prohibits application.
2. **Speckle tracking:** Uses coherent amplitude data (complex or magnitude). *Advantage*: Works also where no obvious amplitude features exist. No need for unwrapping. *Disadvantage*: Coherence required, but gaps due to lack of coherence can be bridged.
3. **Coherence tracking**: Uses templates in coherence images and looks for maximum value. Method and possibilities similar to method (2).

Typical achievable accuracy in displacement: ~ 0.2 pixels in x and y. Errors depend on co-registration, type of features, quality of matching

Processing Line for Offset Tracking

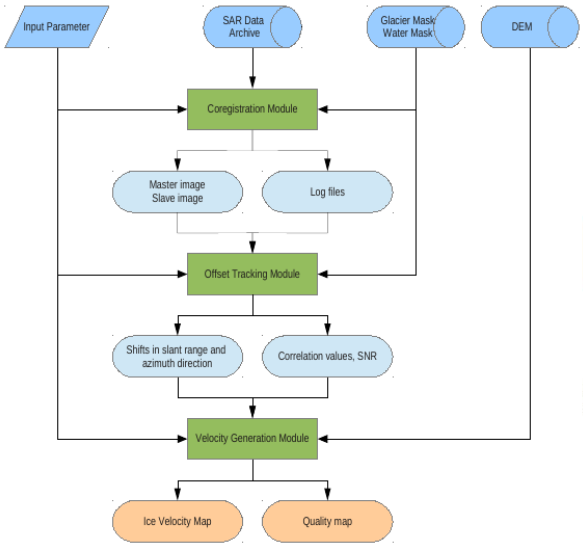

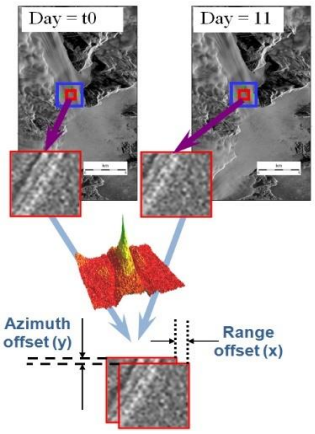

Ice Motion: Comparison InSAR – Offset Tracking

	INSAR	OFFSET TRACKING
Velocity component	LOS motion only	2 motion components LOS (range) **and** along track
Typical time interval (Δt)	6, 12 days Sentinel-1 11 days TSX	11, 22,.. days for TerraSAR-X 6, 12, ... days for Sentinel-1
Typical accuracy of displacement, single pair S1 IW mode, **TerraSAR-X**	≤ 5 mm LOS (Sentinel-1 IW mode, S1)	~0.5 m, ~ **0.2 m** slant range ~1.0 m, ~ **0.2 m** along track
Main constraints	Temporal decorrelation (lack of coherence) No sensitivity to motion along track Unwrapping problem in case of gaps	Lack of stable amplitude features (for amplitude corr.) Coherence (speckle tracking) Lower sensitivity than InSAR (but longer Δt improves accuracy of velocity) Less spatial detail

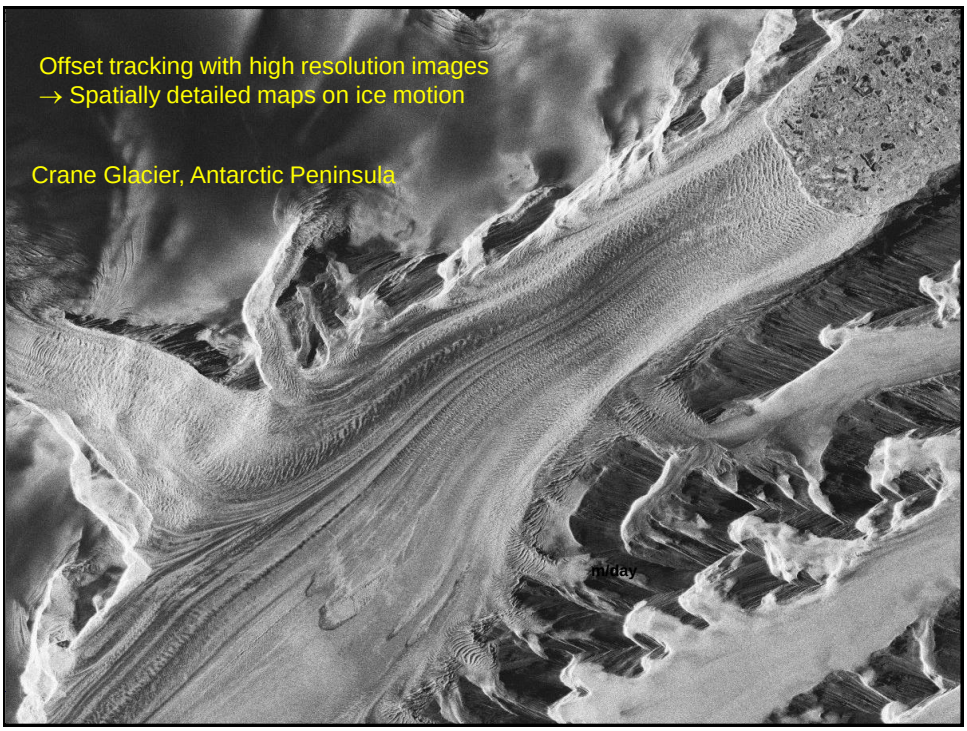

Study on Mass Balance of Antarctic Peninsula Glaciers by Input-Output Method

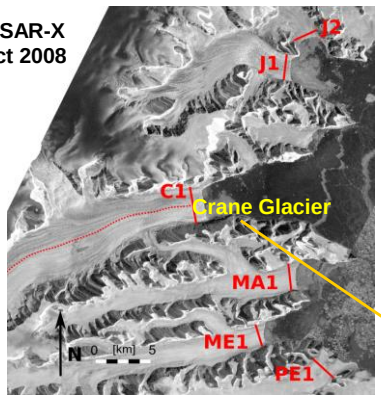

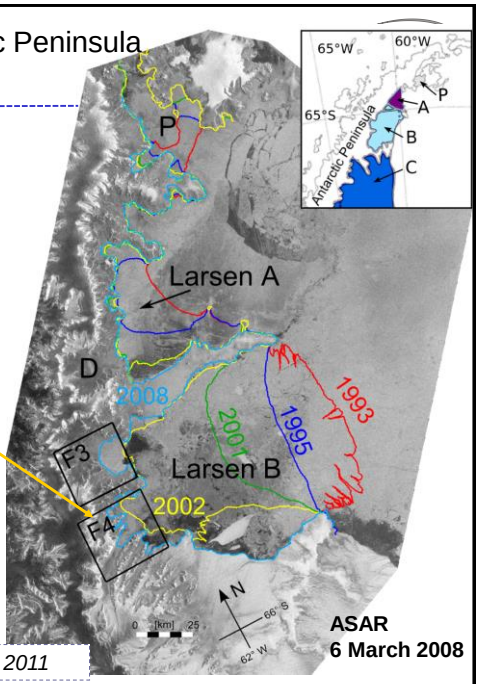

Net mass balance: B_n = SMB - B_{CV}

Estimate of SMB:

In pre-collapse period (previous to 2002) the glacier was in equilibrium; SMB = B_{CV}

Ref: Rott et al. 2011

Study on Acceleration and Mass Budget of Crane Glacier

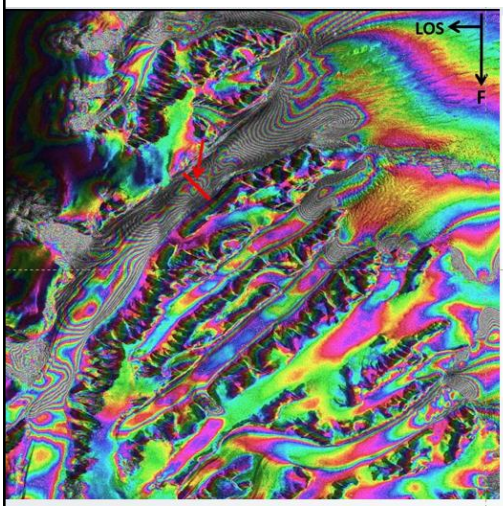

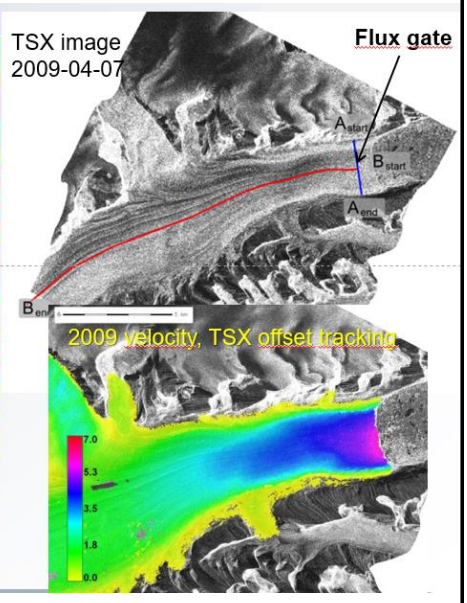

ERS Tandem InSAR 1995/10/31-1995/11/01
Glacier in balanced state, B_A = B_C

Crane Glacier: Retrieval of Calving Flux & Mass Balance
ERS InSAR (1995/1999), TerraSAR-X (2007 - 2015)

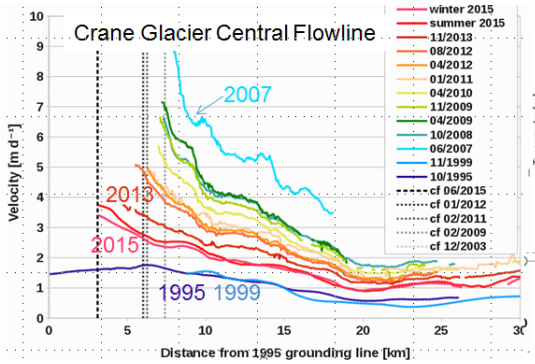

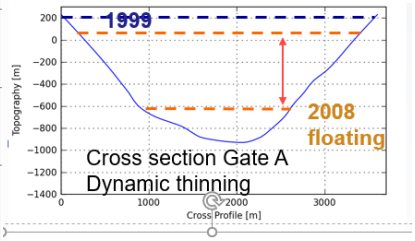

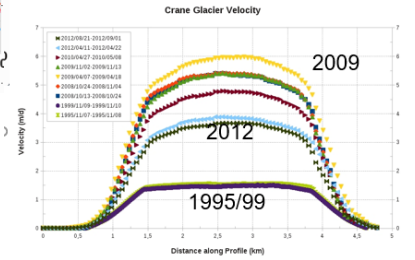

Date	Flux Gt/yr	B_n Gt/yr
1995-99	1.15 (= B_A)	Balance Flux
June 2007	5.02	-3.87
2008-09	2.92	-1.77
Nov. 2013	1.72	-0.58
Summer 2015	1.42	-0.27
Winter 2015	1.36	-0.21

Ref: Wuite et al. 2015

ENVEO Products on Flow Velocity of Ice Sheets and Ice Caps

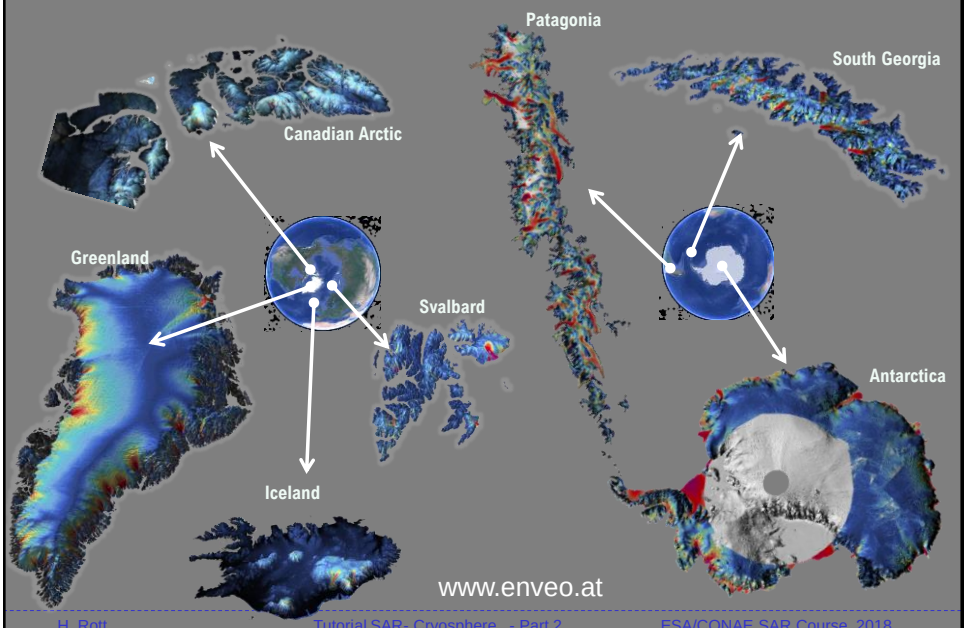

Sentinel-1 Products on Ice Velocity – Time Series

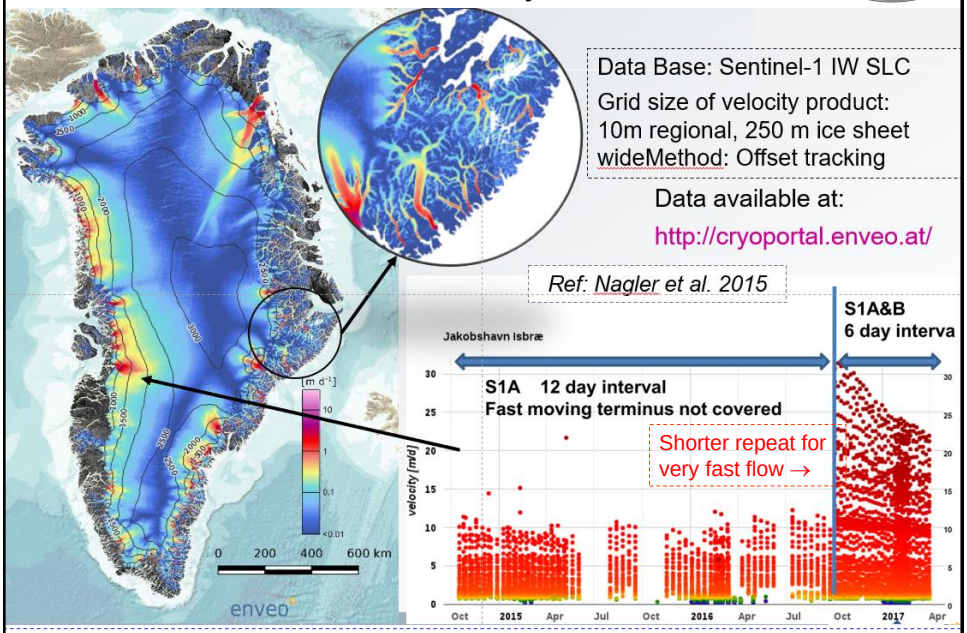

3D Surface Deformation and Glacier Hydraulics

The ice flow varies in time due to

- **Changes at bedrock (e.g. geothermal heat flow, sub-glacial volcanism) or of frontal back-stress (retreat of grounding line)**
- **Seasonal variations in dependence of internal water pressure**
- **Outbreaks of sub-glacial lakes**
- **Surges (dynamic instability causing rapid glacier advances)**
- **Decrease of glacier volume (due to increased melt)**

In case of rapid changes of ice velocity and topography (e.g. due to water outbreaks – jökulhlaups, or glacier surges) single-track SAR repeat pass data are lacking essential information**.**

- **SP-InSAR is able to provide rapidly updated DEMs**
- **Options for measuring 3D velocity vector:**
  - **Offset tracking: Images of 2 crossing orbits**
  - **Repeat-pass InSAR: Images from 3 different view directions**

Retrieval of 3D Ice Motion by SAR Offset Tracking

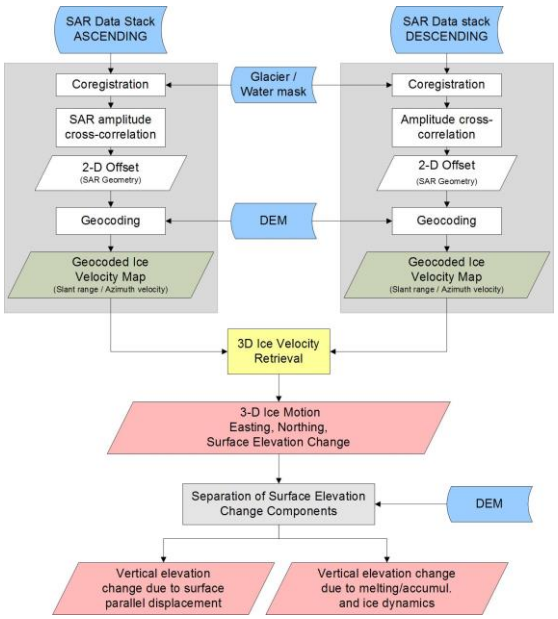

Offset tracking:

Data from ascending & descending orbits deliver 4 different projections of the velocity vector

High resolution SAR image data needed to obtain good sensitivity for vertical displacement

Study on 3D Ice Motion & Glacier Hydraulics, Greenland

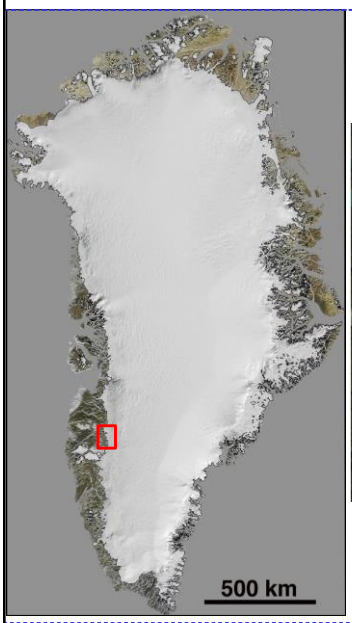

K-transect at 67° N

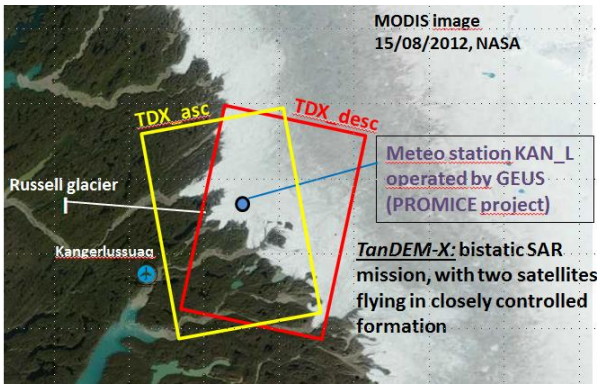

SAR Data for 3D Ice Motion

TDX repeat pass image pairs of ascending & descending orbits:

4 projections of the displacement vector:

ΔLOS + ΔAlong-track, (*Asc* + *Desc*) → 3D Displacement

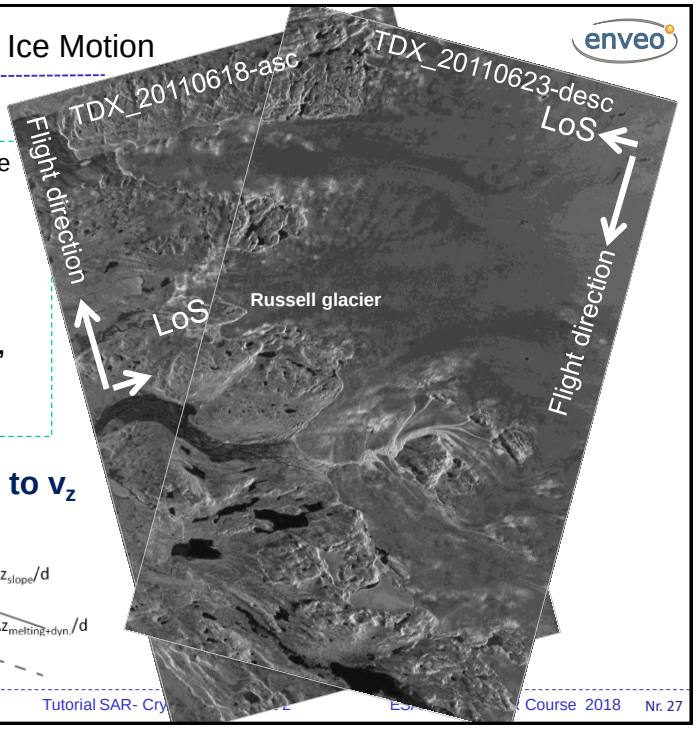

Contributions to v_z

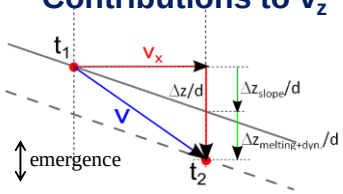

Surface Elevation Change by SP-InSAR DEM Differencing

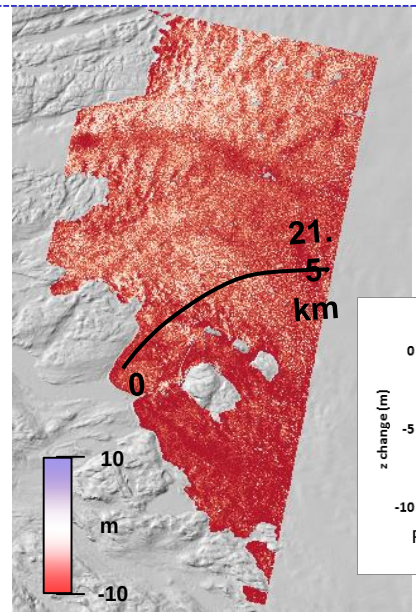

Seasonal elevation change June to September 2011 by DEM differencing

DEMs:

- TanDEM-X DEM 12/06/2011
- TanDEM-X DEM 08/09/2011

Includes: elevation change due to

- ***Surface melt***
- ***Ice flow dynamics***

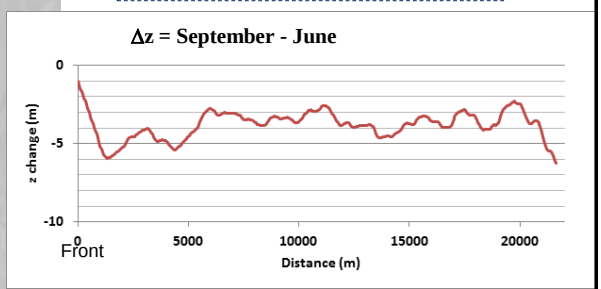

Horizontal and Vertical Displacement Rates

Horizontal flow velocity along centre line

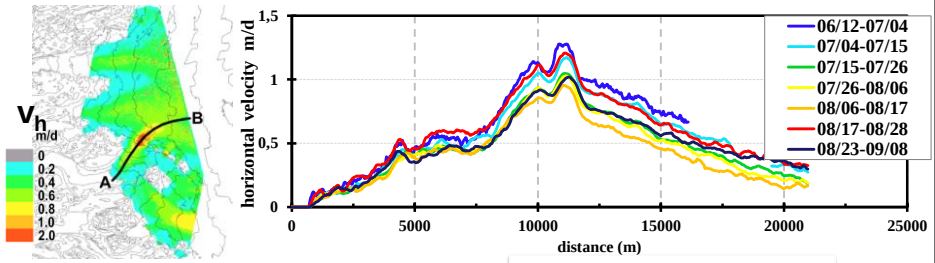

Vertical displacement rates along centre line

Uplift and acceleration in late August related to rainfall

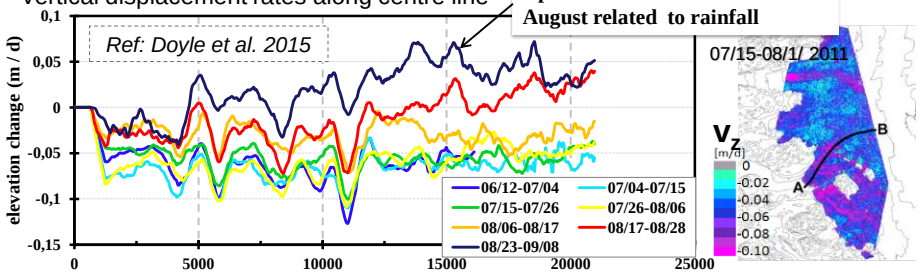

Vertical Displacement and Glacier Drainage

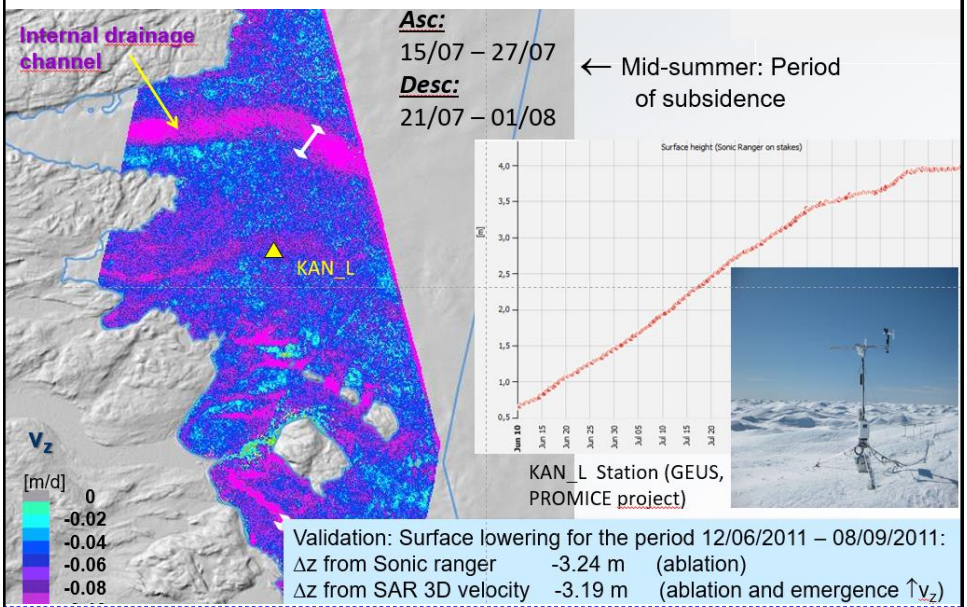

Asc:
15/07 – 27/07
Desc:
21/07 – 01/08

← Mid-summer: Period of subsidence

Validation: Surface lowering for the period 12/06/2011 – 08/09/2011:
Δz from Sonic ranger -3.24 m (ablation)
Δz from SAR 3D velocity -3.19 m (ablation and emergence ↑v_z)

Single-Pass InSAR Application for Monitoring Surface Elevation Change and Mass Balance

The change in glacier surface elevation and volume ΔV over time interval Δt can be converted into change of glacier mass, **net mass balance, B_N**:

$$B_n(\Delta t) = \int_S \rho \, \Delta h_s(\Delta t) ds$$

for glacier ice: ρ = 900 kg m^{-3}

B_N is a key parameter for climate research and hydrology

Regular surveys by single-pass InSAR DEMs offer excellent capabilities to reduce the uncertainty in global glacier mass balance: **DEM-differencing**

SAR signal penetration (position of scattering phase center ϕ_z) needs to be considered for DEM differencing. Options:

- Use repeat observations at **same SAR frequency, look angle and snow state** $\Rightarrow$ relative position of ϕ_z below snow surface remains the same
- Use InSAR DEM data acquired over **wet snow surfaces**
- Estimate and correct penetration **for given snow state and SAR frequency** (using model and/or empirical data)

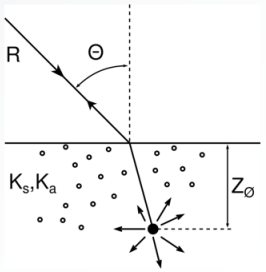

Elevation Difference ICESat TanDEM-X DEM

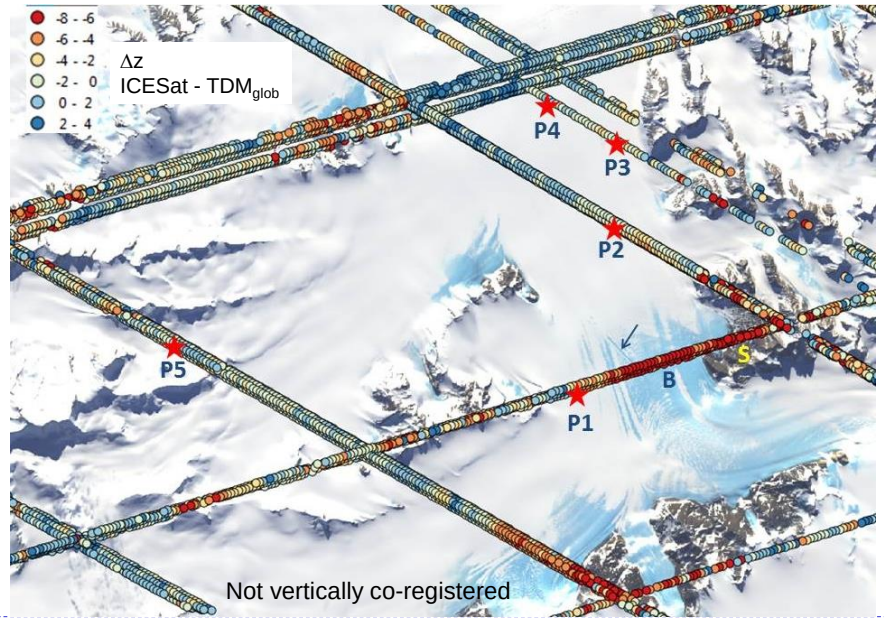

Reference surfaces for vertical co-registration (no penetration for SAR)

← Ice-free slope

↓ Blue ice field

Mean offsets ICESat – TDM
Ice-free slope & Blue ice

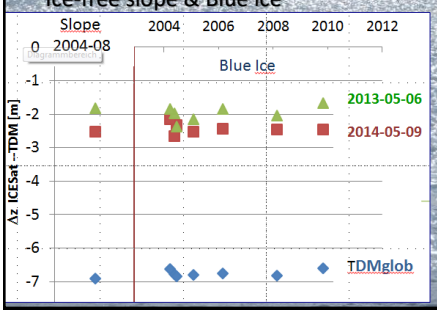

Differences in Stratigraphy and Penetration

Differences in wind exposure affect snow accumulation, metamorphism & penetration

UG near Camp $b_a \approx 150$ mm/yr

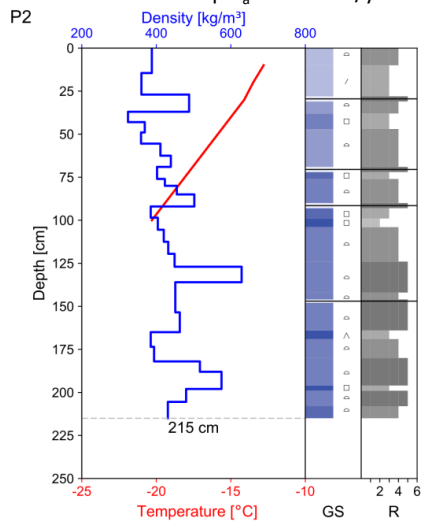

Driscoll Glacier $b_a \approx 350$ mm/yr

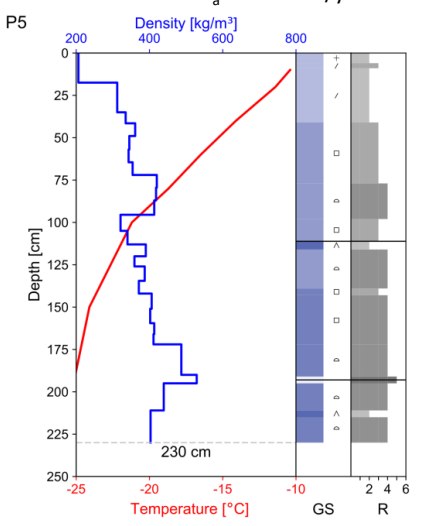

Relations between Coherence and σ° and Penetration Bias

Volume coherence (γ_{vol}) and σ°(hh) at snow pit sites, TDM 2013-05-06 and 2014-05-09

γ(vol) is derived from total normalized coherence which includes the following contributions:

γ(tot) = γ(SNR) × γ(Quant) × γ(Amb) × γ(RG) × γ(Az) × γ(vol)

Δh_b = h(ICESat) – h(TDM) co-registered

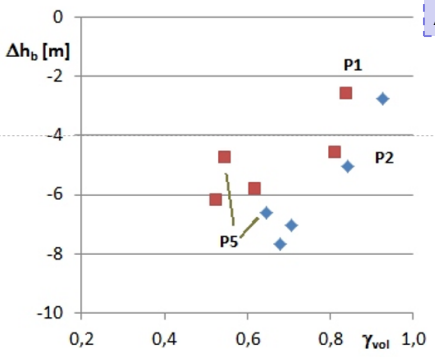

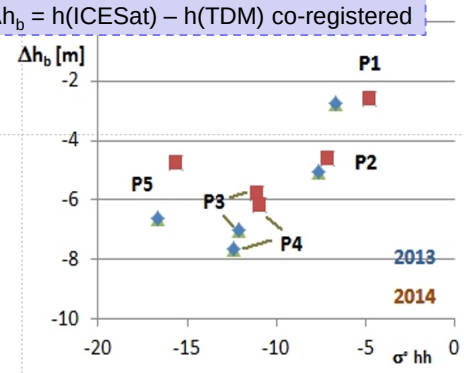

Lower γ_{vol} in 2014, due to larger InSAR baseline

γ and σ° can be used for estimating Δh_b

P1: Near runway. P5: High accumulation rate, on slanting surface above main glacier

Validation of TanDEM-X DEM Differencing Products

Data sets: Surface Elevation Change (dh/dt) 2011 – 2016, Larsen Outlet Glaciers

- TDM CoSSC data for DEMs were acquired from same satellite track in winter (frozen snow/ice) → **data sets with same σ° and same incidence angle**
- Comparison with airborne lidar (ATM) data of NASA IceBridge, Nov. 2011-Nov. 2016, acquired along central flowlines of several glaciers
- Both data sets independently processed

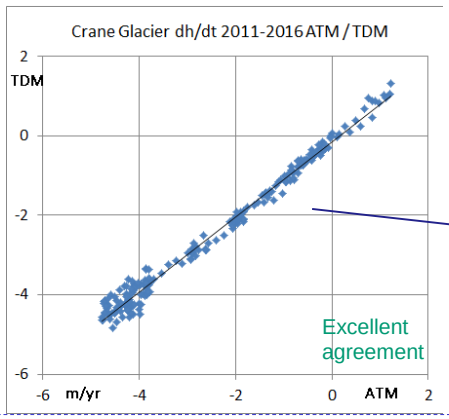

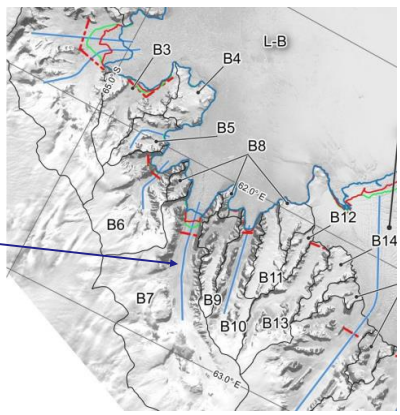

Spatially Detailed Analysis of Glacier Volume Change and Mass Balance by TanDEM-X – Larsen B Outlet Glaciers

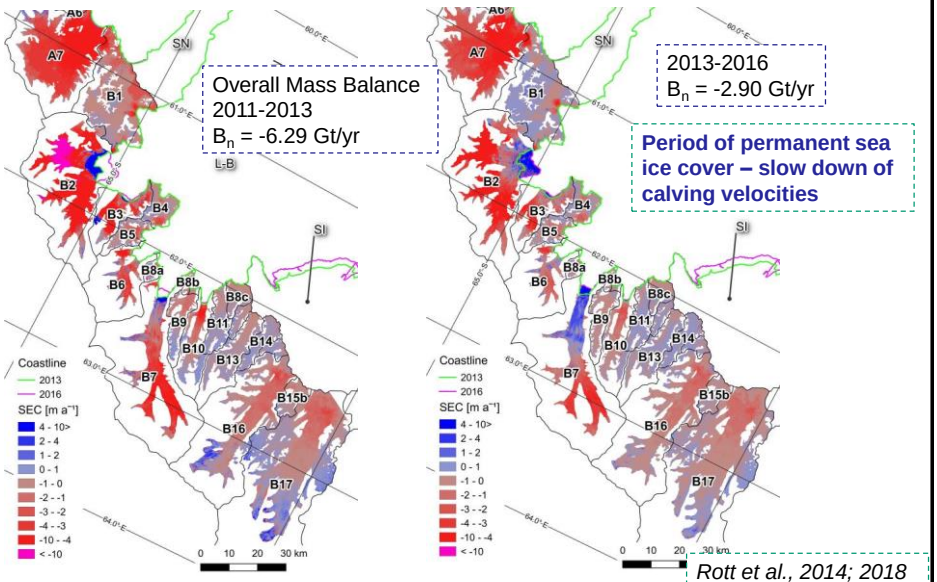

Major Differences in Downwasting of Different Glaciers

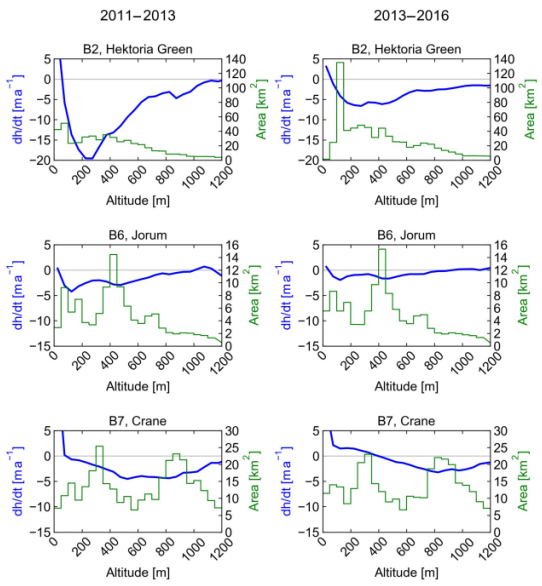

TerraSAR-X image, Green and Hektoria glaciers. Ice front 2013-06-20 (yellow) and 2016-07-27 (red).

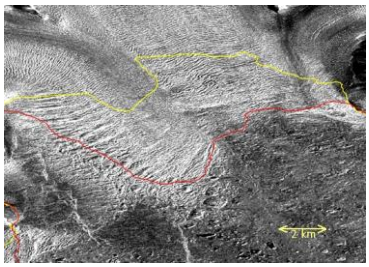

Advance of glacier front 2013 to 2016, glacier terminus is floating.

Mass Balance of Patagonia Glaciers – the Classical Method

Stuefer et al., 2007

Mass Balance by Tandem-X DEM Differencing

dh/dt 2000-2012 | 2012-2016 | elevation

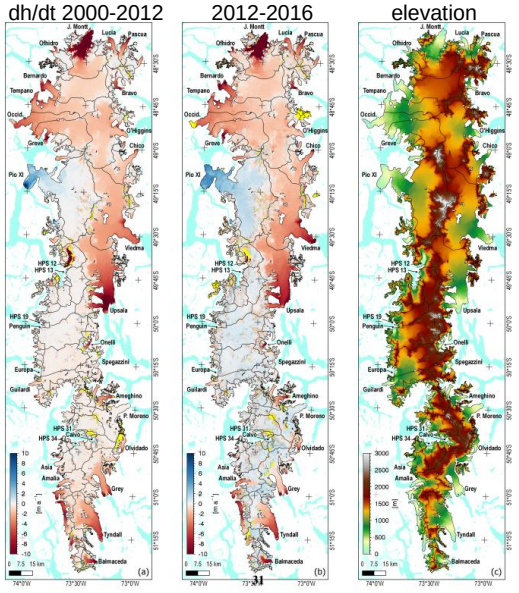

Different behaviour of individual glaciers

Upsala

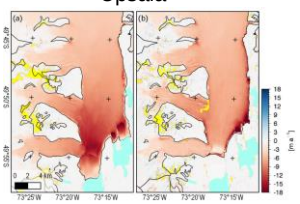

Pio XI

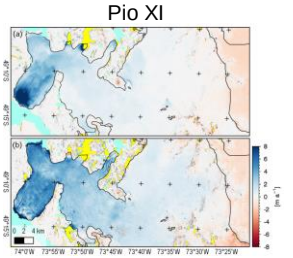

Ref. Abdel Jaber, 2016 and ESA Project SAMBA by DLR-IMF & ENVEO

Advanced Techniques: 3D Glacier Tomography by InSAR

TomoSAR geometry

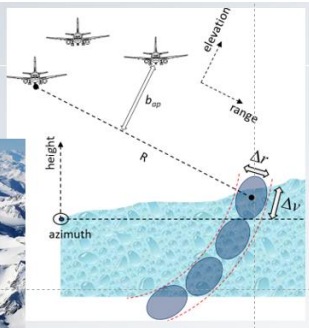

Mittelbergferner, Ötztal Alps

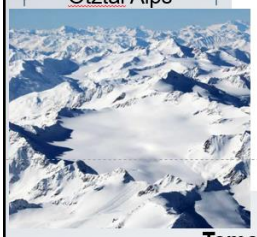

AlpTomoSAR Campaign

L-Band airborne SAR images of 20 parallel tracks are coherently combined to obtain 3-D tomographic SAR (TomoSAR) cubes. Each volume element (voxel) represents radar reflectivity from a location in the 3-D space at spatial resolution of meters.

Tebaldini et al., IEEE TGRS 2016

TomoSAR image in 25 m depth

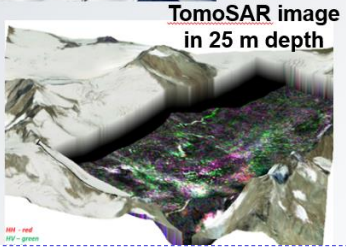

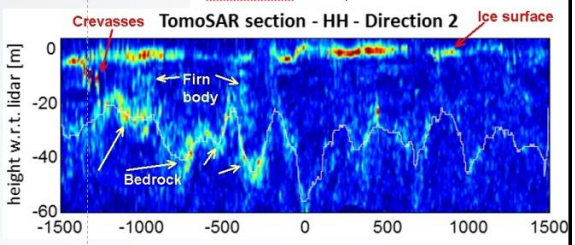

References

- Abdel Jaber, W. Derivation of mass balance and surface velocity of glaciers by means of high resolution synthetic aperture radar: application to the Patagonian Icefields and Antarctica, Doct. Thesis, Technical Univ. Munich, DLR Res. Report 2016-54, 236 pp, 2016.
- Doyle, S., Hubbard, A., et al. 2015. Amplified melt and flow of the Greenland ice sheet driven by late-summer cyclonic rainfall. *Nature Geosc*. doi:10.1038/ngeo2482
- Magnússon, E., H. Rott, H. Björnsson and F. Pálsson. 2007. The impact of jökulhlaups on basal sliding observed by SAR interferometry on Vatnajökull *J. Glaciol.,* 53 (181), 232-240.
- Nagler, T., Rott, H., Hetzenecker, M., Wuite, J., Potin, P. 2015. The Sentinel-1 Mission: New opportunities for ice sheet observations. *Remote Sens.*, 7, 9371-9389.
- Nagler, T., H. Rott, M. Hetzenecker, et al. 2012. Retrieval of 3D glacier movement by means of high resolution X-band SAR data. Proc. IGARSS-2012, pp. 3233-3236.
- Rott, H., Müller, F., Nagler, T., Floricioiu D. 2011. The imbalance of glaciers after disintegration of Larsen B ice shelf, Antarctic Peninsula. *The Cryosphere*, 5, 125-134.
- Rott, H., Floricioiu, D., Wuite, J., et al. 2014. Mass changes of outlet glaciers along the Nordensjköld Coast, northern Antarctic Peninsula, based on TanDEM-X satellite measurements. *Geophys. Res. Lett*., 41, 8123-8129.
- Rott, H., Abdel Jaber, W., Wuite, J., et al., 2018. Changing pattern of ice flow and mass balance for glaciers discharging into the Larsen A and B embayments, Antarctic Peninsula, 2011 to 2016. *The Cryosphere*, 12, p.1273-1291.
- Stuefer, M., H. Rott, P. Skvarca. 2007. Glaciar Perito Moreno, Patagonia: Climate sensitivities and glacier characteristics preceding the 2003/2004 and 2005/2006 damming events. *J. Glaciol*., 53(189), 1.13.
- Tebaldini, S., Nagler, T., Rott, H., Heilig, A. 2016. Imaging the internal structure of an Alpine glacier via L-Band airborne SAR tomography. *IEEE Trans. Geosc. Rem. Sens*., 54(12), 7197-7209, doi: 10.1109/TGRS.2016.2597361.
- Wuite, J., Rott, H., et al. 2015. Evolution of surface velocities and ice discharge of Larsen B outlet glaciers from 1995 to 2013. *The Cryosphere*, 9, 957-969.